Supplemental Data

Transient Receptor Potential Vanilloid 4 (TRPV4) Activation by Arachidonic Acid Requires Protein Kinase A-Mediated Phosphorylation

Sheng Cao, Andriy Anishkin, Natalya S. Zinkevich, Yoshinori Nishijima, Ankush Korishettar, Zhihao Wang, Juan Fang, David A. Wilcox, and David X. Zhang

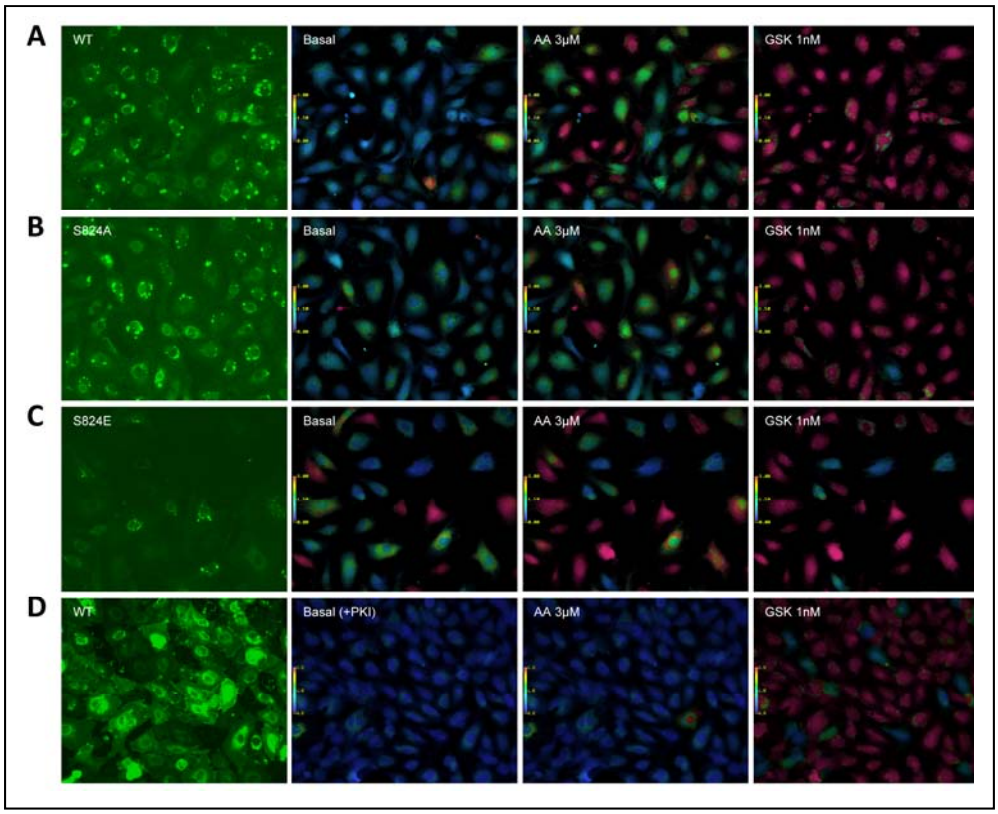

FIGURE S1. Regulation of AA-induced TRPV4 activation by S824 phosphorylation and PKA in HCAECs. A-D, Representative images of GFP fluorescence (left) and fura-2 calcium assay (right 3 panels) of HCAECs transfected with TRPV4 (C-terminal GFP fusion protein) wild-type (WT), S824A or S824E mutants in a lentiviral vector. Images of GFP fluorescence were first acquired before any treatments for the subsequent fura-2 calcium assay. For fura-2 assay, cells were preincubated with vehicle (A-C) or the PKA inhibitor PKI (10 μM) for 30 min (D), rinse out free PKI in the bath and treated sequentially with AA (3 μM), and the synthetic TRPV4 activator GSK 1016790A (GSK; 1 nM). Note that the image of GFP fluorescence in panel B was reused in Fig 2A to illustrate the cell membrane expression of TRPV4-GFP S824 mutants in HCAECs.

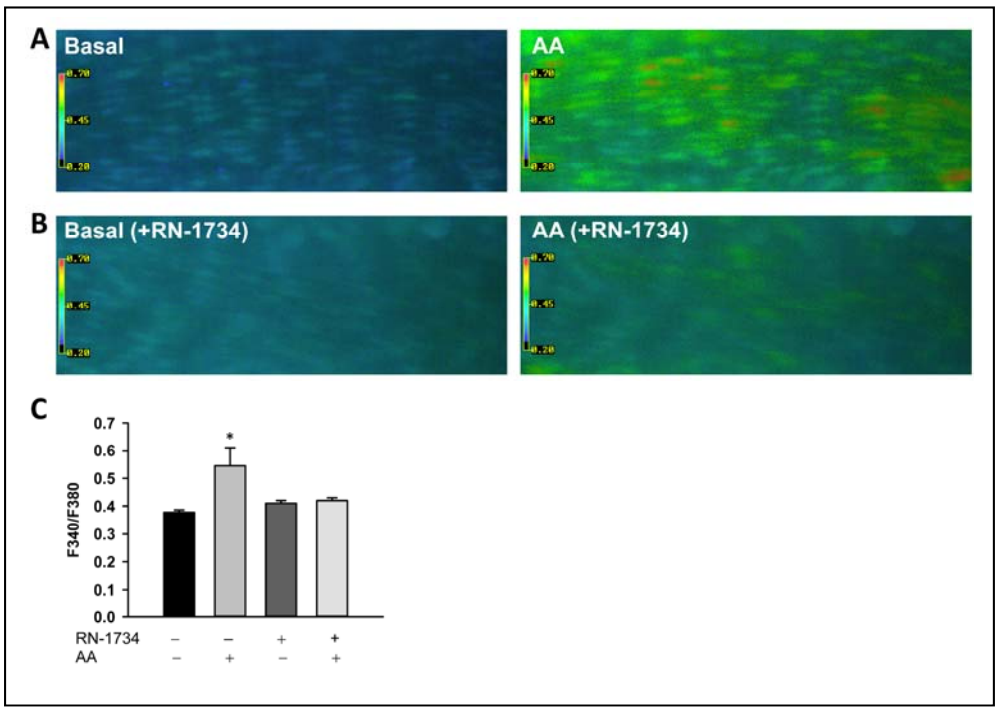

FIGURE S2. AA-induced and TRPV4-mediated Ca^{2+} response in native endothelial cells in situ of human coronary arteries. Coronary arteries were freshly isolated from cardiac surgical specimen and endothelial cells were loaded with fura-2 AM for intracellular Ca^{2+} imaging. A-B, Representative images of endothelial Ca^{2+} responses to AA (1 μM) in an artery pretreated with vehicle (Control) or RN-1734 (20 μM), a TRPV4-selective channel blocker. C, Summarized data of endothelial $[Ca^{2+}]_i$ increase. *P ≤ 0.05 compared with basal. Data represent mean ± SEM of 2-4 tissues for each group, with 30-50 endothelial cells analyzed per each artery.

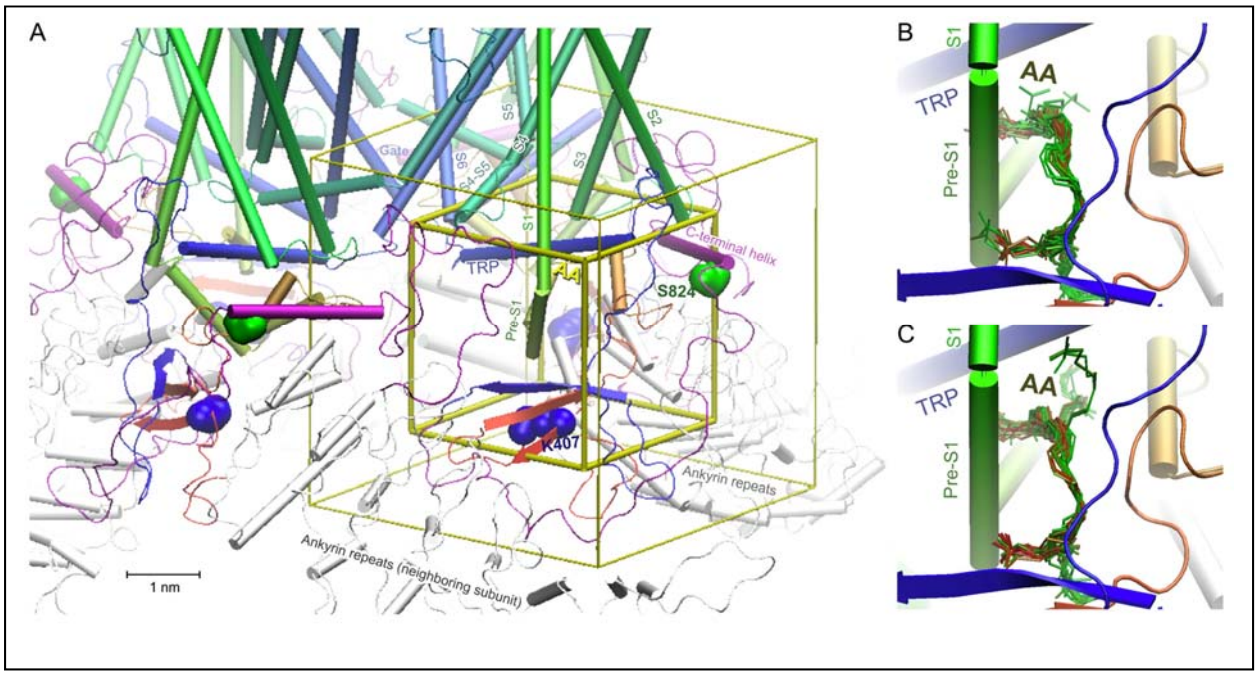

FIGURE S3. Exploration of a possible binding site for AA using automated docking. Earlier studies indicate that TRP helix functions as a "force hub" for multiple mechanical inputs, integrating various stimuli and controlling the expansion of the channel gate (1,2). In addition, residue K407 (belonging to the putative ARS) is likely implicated in binding or activation of the TRPV4 by AA. Based on that, we hypothesize that AA binds somewhere in the region between TRP helix and K407. To visualize a likely binding position and conformation for AA, we have used AutoDock Vina (3). A, We have set up the search box for the center of AA to cover the location from TRP helix and K407 (a 3-nm box shown with thick yellow tubes), whereas the carboxyl group or aliphatic tail of AA could reach ~1 nm larger region (shown with thin yellow tubes). B, For the homology model with externally docked C-terminal helix, the top 5 predicted AA binding conformations for 10 independent replicate runs are shown as thin bonds, colored from red (most favorable) to green (less favorable). The predominant binding mode is with aliphatic tail of AA located under TRP helix, while the head group is close to K407. C, With the same conditions, the predictions for the homology model with C-terminal helix docked inside the cytoplasmic vestibule of TRPV4 bring similar expected conformations for the bound AA.

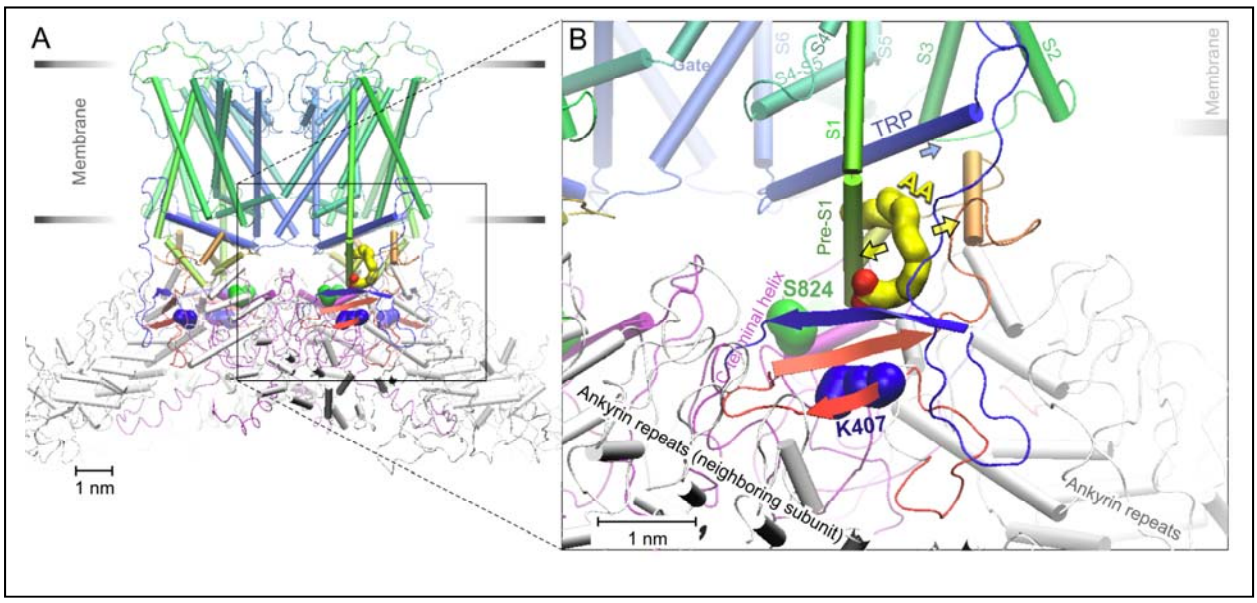

FIGURE S4. An alternative modeled docking position of C-terminal helix containing S824. Based on the analysis of human TRPV4 homology model and the predicted conformations of C-terminal domain, we suggest that there might be an alternative docked conformation of C-terminal domain inside the cytoplasmic vestibule of the channel. In this conformation as well, C-terminal helix would hinder the expansion of the hydrophobic crevice and channel activation by AA, and also could prevent the access of AA into the crevice. S824 phosphorylation could prevent this docking and sensitize the channel to AA.

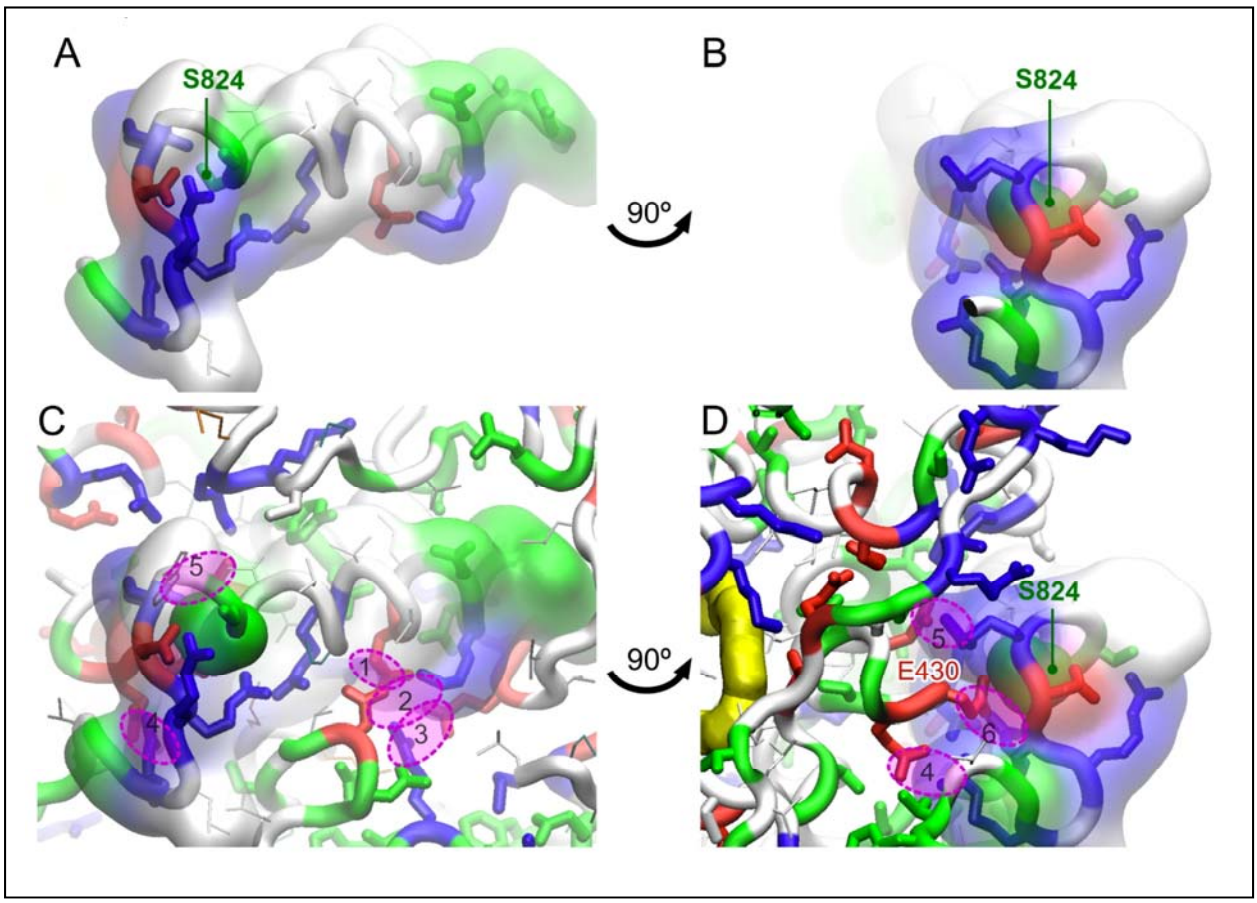

FIGURE S5. Structural determinants of the C-terminal S824 helix binding at the external position. Side (A) and front (B) views of the isolated helix illustrate the pattern of the residue properties, with basic amino acids (blue) abundant in the vicinity of S824, a non-polar patch (white) present at the top, and a few polar residues (green) mostly located at the end of the helix. The translucent surface approximates solvent-accessible boundary of the domain. When docked at the "external" position (C, D) under S2-S3 loop, the alpha-helix is able to form several salt bridges (marked with magenta outlines) to the residues at the channel region, while the non-polar patch could establish hydrophobic interactions with the residues of S2-S3 loop.

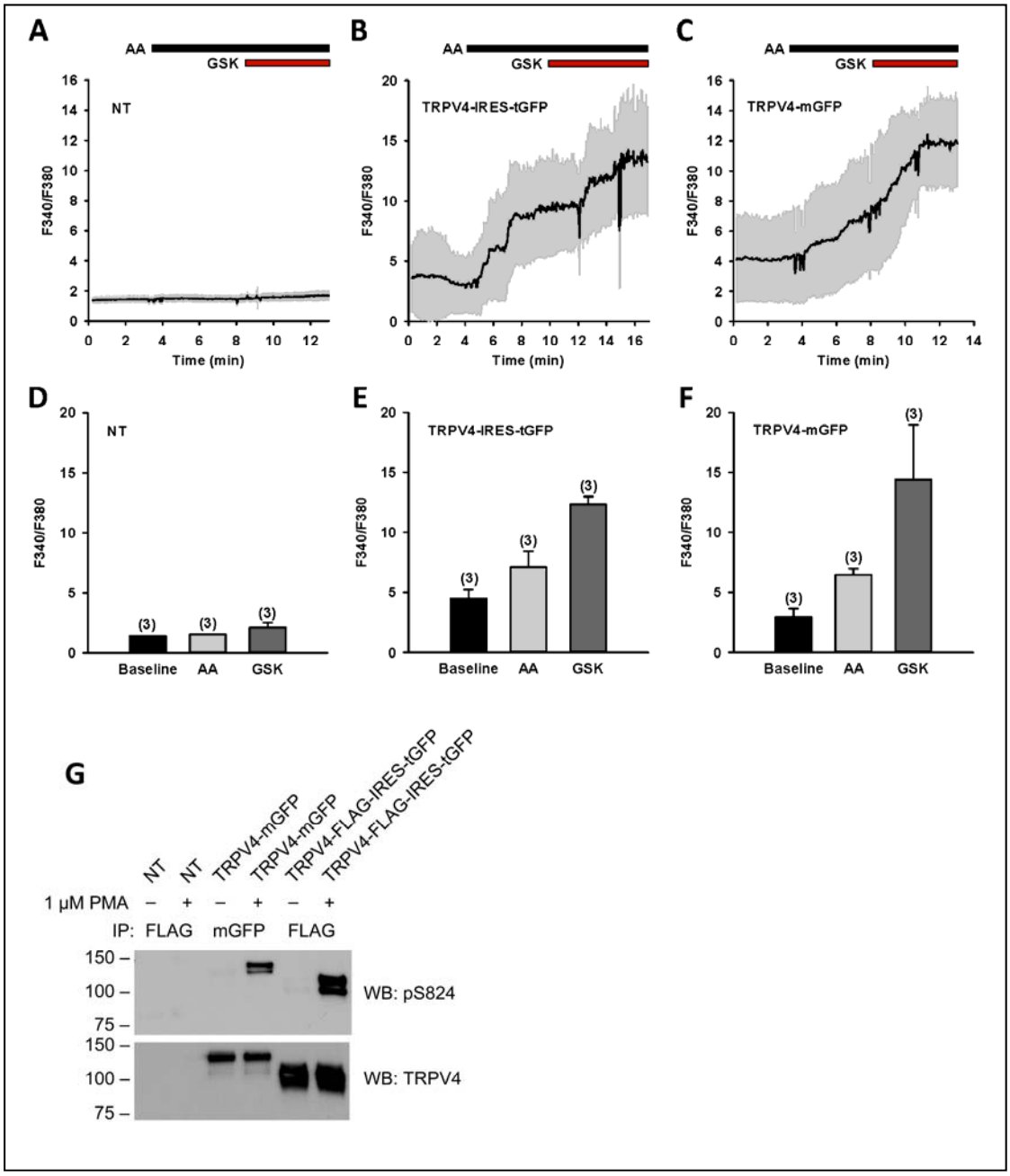

FIGURE S6. TRPV4-mediated Ca^{2+} response and phosphorylation at S824 in HEK 293 cells overexpressing human TRPV4. HEK 293 cells were transiently transfected with pCMV6 plasmids encoding TRPV4-FLAG-IRES-turbo GFP (TRPV4-FLAG-IRES-tGFP) or TRPV4-mGFP. NT indicates non-transfected cells. A-C, representative traces of fura-2 calcium assay. The black line denotes mean F340/F380 ratio and gray area 1× standard deviation. Cells were treated sequentially with AA (6 μM) and the synthetic TRPV4 activator GSK1016790A (GSK; 3 nM). D-F, Summarized data for AA- and GSK-induced Ca^{2+} responses (F340/F380). All summarized data represent mean ± SEM, with the number of independent experiments indicated in brackets above error bars. G, TRPV4 phosphorylation at S824. Cells were exposed to the PKC activator PMA (1 μM) for 5 min, followed by the protein phosphatase (PP) 1/2A inhibitor cantharidin (10 μM) for 2 min. TRPV4 S824 phosphorylation was analyzed by Western blotting with a phosphoserine motif antibody against the motif RXRXXS*/T* (pS824 antibodies), and the same blot was reprobed with anti-TRPV4 antibodies (Abcam; ab39260) to detect total cellular TRPV4 proteins.

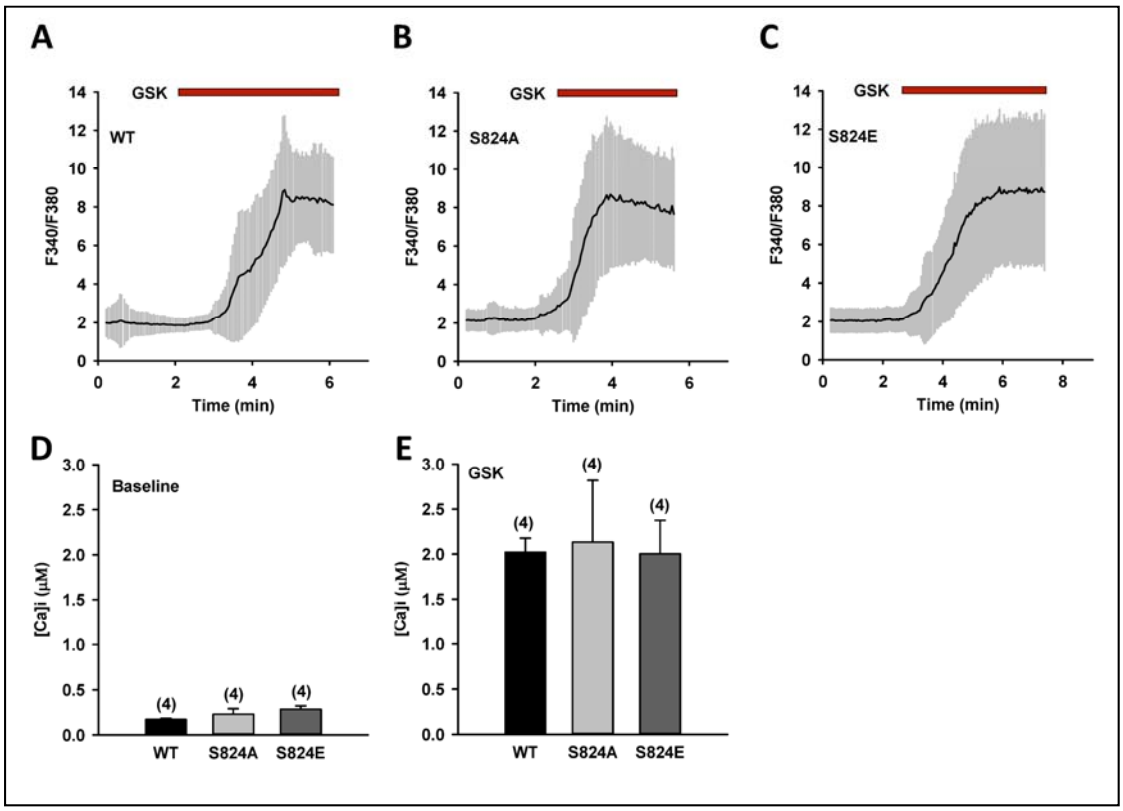

FIGURE S7. TRPV4-mediated Ca^{2+} response in HCAECs using a lower affinity Ca^{2+} indicator, fura-4F. A-C, Representative traces of changes in F340/F380 ratio with time in HCAECs transduced with wild-type (WT) TRPV4 (C-terminal GFP fusion protein), S824A or S824E mutants cloned into a lentiviral vector. Cells were treated with the synthetic TRPV4 activator GSK1016790A (GSK; 1 nM). The black line denotes mean F340/F380 ratio and the gray area 1× standard deviation. D-E, Summarized data for intracellular calcium concentrations ($[Ca^{2+}]_i$) at baseline and after GSK treatment in WT, S824A and S824E mutants. All data represent mean ± SEM, with the number of independent experiments indicated in brackets above error bars.

REFERENCES

1. Teng, J., Loukin, S. H., Anishkin, A., and Kung, C. (2015) L596-W733 bond between the start of the S4-S5 linker and the TRP box stabilizes the closed state of TRPV4 channel. *Proc. Natl. Acad. Sci. U. S. A.* **112**, 3386-3391
2. Teng, J., Loukin, S. H., Anishkin, A., and Kung, C. (2016) A competing hydrophobic tug on L596 to the membrane core unlatches S4-S5 linker elbow from TRP helix and allows TRPV4 channel to open. *Proc. Natl. Acad. Sci. U. S. A.* **113**, 11847-11852
3. Trott, O., and Olson, A. J. (2010) AutoDock Vina: Improving the speed and accuracy of docking with a new scoring function, efficient optimization, and multithreading. *J. Comput. Chem.* **31**, 455-461